Hydrol. Earth Syst. Sci., 21, 5111–5126, 2017
https://doi.org/10.5194/hess-21-5111-2017

Hydrology and Earth System Sciences
Open Access
EGU

Snow cover dynamics in Andean watersheds of Chile (32.0–39.5° S) during the years 2000–2016

Alejandra Stehr[1,2] **and Mauricio Aguayo**[1,2]

[1]Centre for Environmental Sciences EULA-CHILE, University of Concepción, Concepción, Chile
[2]Faculty of Environmental Sciences, University of Concepción, Concepción, Chile

Correspondence to: Alejandra Stehr (astehr@udec.cl)

Received: 15 July 2016 – Discussion started: 20 September 2016
Revised: 18 June 2017 – Accepted: 18 August 2017 – Published: 11 October 2017

Abstract. Andean watersheds present important snowfall accumulation mainly during the winter, which melts during the spring and part of the summer. The effect of snowmelt on the water balance can be critical to sustain agriculture activities, hydropower generation, urban water supplies and wildlife. In Chile, 25 % of the territory between the region of Valparaiso and Araucanía comprises areas where snow precipitation occurs. As in many other difficult-to-access regions of the world, there is a lack of hydrological data of the Chilean Andes related to discharge, snow courses, and snow depths, which complicates the analysis of important hydrological processes (e.g. water availability). Remote sensing provides a promising opportunity to enhance the assessment and monitoring of the spatial and temporal variability of snow characteristics, such as the snow cover area (SCA) and snow cover dynamic (SCD). With regards to the foregoing questions, the objective of the study is to evaluate the spatiotemporal dynamics of the SCA at five watersheds (Aconcagua, Rapel, Maule, Biobío and Toltén) located in the Chilean Andes, between latitude 32.0 and 39.5° S, and to analyse its relationship with the precipitation regime/pattern and El Niño–Southern Oscillation (ENSO) events. Those watersheds were chosen because of their importance in terms of their number of inhabitants, and economic activities depending on water resources. The SCA area was obtained from MOD10A2 for the period 2000–2016, and the SCD was analysed through a number of statistical tests to explore observed trends. In order to verify the SCA for trend analysis, a validation of the MOD10A2 product was done, consisting of the comparison of snow presence predicted by MODIS with ground observations. Results indicate that there is an overall agreement of 81 to 98 % between SCA determined from ground observations and MOD10A2, showing that the MODIS snow product can be taken as a feasible remote sensing tool for SCA estimation in southern–central Chile. Regarding SCD, no significant reduction in SCA for the period 2000–2016 was detected, with the exception of the Aconcagua and Rapel watersheds. In addition to that, an important decline in SCA in the five watersheds for the period of 2012 and 2016 was also evident, which is coincidental with the rainfall deficit for the same years. Findings were compared against ENSO episodes that occurred during 2010–2016, detecting that Niña years are coincident with maximum SCA during winter in all watersheds.

1 Introduction

Snowmelt-driven watershed systems are highly sensitive to climate change, because their hydrologic cycle depends on both precipitation and temperature, and because water is already a scarce resource subject to ever-increasing pressure for its use (Barnett et al., 2005; Vicuña et al., 2011; Meza et al., 2012; Valdés-Pineda et al., 2014). Snowmelt controls the shape of the annual hydrograph, and affects the water balance at monthly and shorter timescales (Verbunt et al., 2003; Cortés et al., 2011). The effect of snowmelt on the water balance can be critical to sustain agriculture activities, hydropower generation, urban water supply and wildlife habitat quality (e.g. Vicuña et al., 2012, 2013).

The Andean watersheds present an important snowfall accumulation mainly during the austral winter; snow melts during spring and usually also during part of the summer, depending on relative altitude and ambient temperature. At higher elevations, a snowpack stores significant volumes of

water, which are released to the surface runoff and groundwater when solar radiation increases.

In particular, 25 % of the Chilean territory between the Valparaiso and Araucanía regions is contained in areas where snow precipitation occurs (DGA, 1995). As in many other difficult-to-access regions of the world, the Chilean Andes – unlike western North America or the European Alps – have limited availability in temporal and spatial extent of hydrological data like discharge data, snow courses, and snow depths (Ragettli et al., 2013), which complicates the analysis of important hydrological processes and the validation of water quantity prediction models.

In this regard, remote sensing provides a promising opportunity to enhance the assessment and monitoring of the spatial and temporal variability of different variables involved in the precipitation–runoff processes in areas where data availability for hydrological modelling is scarce (Simic et al., 2004; Boegh et al., 2004; Melesse et al., 2007; Montzka et al., 2008; Milzowa et al., 2009, Er-Raki et al., 2010; Stehr et al., 2009, 2010).

Satellite-derived SCA from products like NOAA-AVHRR or MODIS can be used to enhance the assessment and monitoring of the spatial and temporal variability of snow characteristics (Lee et al., 2006; Li and Wang, 2010; Marchane et al., 2015; Wang et al., 2015), especially when it is combined with field data and snowpack models (Kuchment et al., 2010).

Specific spectral reflectance of snow (higher reflectance in the visible spectrum, compared to the mid-infrared electromagnetic spectrum) allows SCA to be accurately discriminated from snow-free areas using optical remote sensing methods (in the absence of clouds or vegetation canopies). Compared with other remote sensing techniques such as microwaves – which can be used to map snow water equivalent (SWE) – optical remote sensing, which is used to map snow areal extent (SAE), has a much higher spatial resolution (Zhou et al., 2005; Zeinivand and De Smedt, 2009).

Previous a Previous studies have compared MODIS snow maps with ground observations and snow maps produced by the National Operational Hydrologic Remote Sensing Center, USA (NOHRSC) (Hall et al., 2002; Klein and Barnett, 2003; Tekeli et al., 2005; Aulta et al., 2006). Klein and Barnett (2003) compared MODIS and NOHRSC products with ground observations (SNOTEL measurements), obtaining an overall accuracy of 94 and 76 %, respectively. The MOD10A2 snow product is capable of predicting the presence of snow with good precision (over 90 %) when the sky is clear (Zhou et al., 2005; Liang et al., 2008a; Wang et al., 2008; Huang et al., 2011; Zheng et al., 2017). All the previous studies were done in watersheds with a surface topography not as complex as in the Chilean Andes, where we have very steep slopes and a great oceanic effect due to the short distance between the coastline and the mountains.

Many of the studies on SCA changes and variability were done in the Northern Hemisphere, where topographic and orographic conditions are different from the ones we have in Chile. Research studies generally show negative trends in snow cover extent and snow water equivalent across both North America and Eurasia.

In Europe, Krajcí et al. (2016) analysed the main Slovak watersheds; for the 2001–2006 period, they obtained an increase in mean SCA; however, a significantly lower SCA is observed in the next 2007–2012 period. Their results indicate that there is no significant change in the mean watershed SCA in the period 2001–2014. Dietz et al. (2012), in their study of snow cover characteristics in Europe, found some abnormal events when comparing the mean conditions with single snow cover seasons. For the season 2005/2006 in particular, an increased snow cover with a later snow cover melt was detected. Marchane et al. (2015) studied the SCD over the Moroccan Atlas mountain range from 2000 until 2013, concluding that SCA has a strong inter-annual variability and that there is no statistical evidence of a trend in that period.

In Asia, two important regions have been studied: the Tibetan Plateau and the Himalayan region. In the case of the Tibetan Plateau, Zhang et al. (2012) have studied the SCD of four lake watersheds for the period 2001–2010; results indicate that spatial distribution and patterns of snow-covered days are very stable from year to year, and that there is no trend of snow cover change for each watershed. For the same period, Tang et al. (2013) found a high inter-annual variability of SCA, with parts of the studied area showing a declining trend in SCA, and other parts showing increasing trends in SCA. Wang et al. (2015) evaluated trends in SCA, showing a decrease in snow-covered areas from 2003 until 2010. For the Himalayan region, Maskey et al. (2011) studied the trends and variability of snow cover changes above 3000 m during the 2000–2008 period, showing a decreasing trend of snow cover during January and increasing trends during March. Snehmani et al. (2016) studied the 2001–2012 winter period (November–April) in order to obtain clear negative snow cover trends in the basin. Azmat et al. (2017) indicated that the watershed shows a consistent or slightly decreasing trend of snow cover, particularly over the high-altitude parts of the watershed during 2000–2009, and in the 14-year analysis (2000–2013), a slight expansion in the snow-covered area was observed in the whole basin. Gurung et al. (2017), based on the analysis SCA data between 2003 and 2012, also obtained a decline in SCA, with a statistically significant negative correlation between SCA and temperature, which indicates that this trend is partly a result of increasing temperatures.

In North America, Pederson et al. (2013) found that, since 1980, in the northern and southern Rocky Mountains the 1 April snow water equivalent (SWE) has been changing synchronously, and generally declining, associated with springtime warming. Fassnacht and Hultstrand (2015) examined trends in snow depth and SWE from three long-term snow course stations in northern Colorado from 1936 to 2014. They found negative trends at two of the stations for all the

period and, at the third station, a positive trend was found for the first half of the record, and a decrease over the second half. Harpold et al. (2012) analysed SNOTEL SWE for the central and southern Rocky Mountains for the period 1984–2009; they found widespread decreases in maximum SWE and duration of snow cover. After a review of various studies in North America, Kunkel et al. (2016) concluded that all of them are consistent in indicating a decrease in snow on the ground, with some of the most extreme low values occurring in the last 10–15 years.

Studies of snowpack variation done in the central Andes of Chile and Argentina show that the average regional maximum value of the SWE series displays a positive (though non-significant) trend with marked interannual variability ranging from 6 to 257 % of the 1966–2004 mean (Masiokas et al., 2006). Results from Cornwell et al. (2016), who made a SWE reconstruction between 2001 and 2014, indicate that the years 2002 and 2005 stand out for displaying large positive anomalies throughout the entire model domain. The northern part shows above-average accumulation in only 3 out of the 14 simulated years (2002, 2005 and 2007), whereas the other part of the study area shows above-average accumulation for 6 years (2001, 2002, 2005, 2006, 2008 and 2009). In particular, the years 2007 and 2009 show a bimodal spatial structure, with excess accumulation (deficit) in the northern (southern) area and the inverse pattern in the latter year.

From the literature review, it is evident that SCD is site-specific and exhibits high variability among the different sites around the world. The Andes mountain range (on the Chilean side) has a great oceanic effect due to the short distance between the coastal line and the mountains, unlike the Northern Hemisphere, which has a big continental influence. This makes the isotherm 0 higher than in the Northern Hemisphere; in addition, the topographic features characterized by mean heights above 3000 m, with very steep slopes that produce a huge orographic effect that forces the rise of the western winds and condensation of moisture, strongly affect the regime of precipitation and temperatures. This causes small-scale spatial variations in weather, which are sometimes difficult to identify in satellite imagery. All the previously mentioned aspects make it necessary to do a validation of MOD10A2 before using it for other analyses. Indeed, one of the main sources of error in the classification of satellite images is the interpretation of topographic features, especially in areas with rugged slopes. The irregular topography produces shading and lighting effects that change the radiometric response of the surface, which depends on the local slope and its orientation (Riaño et al., 2003). As the climate-controlling hydrologic processes in the Andes are influenced by El Niño events (Escobar and Aceituno, 1993; Ayala et al., 2014), as well as by warm winter storms (Garreaud, 2013), assessment of SCD is of special interest in this region. Pioneer studies have been presented in recent years for the Mataquito River watershed (Demaría et al., 2013; Vicuña et al., 2013). The aim of the study is to evaluate the spatiotemporal dynamics of the SCA in the southern–central Chilean Andes, and to analyse its relationship with the precipitation regime/pattern and El Niño–Southern Oscillation (ENSO) events. To prove this, we selected five watersheds located in the Chilean Andes, between latitude 32.0 and 39.5° S. We investigated trends and variability of snow cover changes at different temporal scales (seasonal and annual) and we used Moderate Resolution Imaging Spectroradiometer (MODIS) snow cover products (Hall et al., 2007) from 2000 to 2017. In situ precipitation measurements from the National General Water Directorate (DGA) were used.

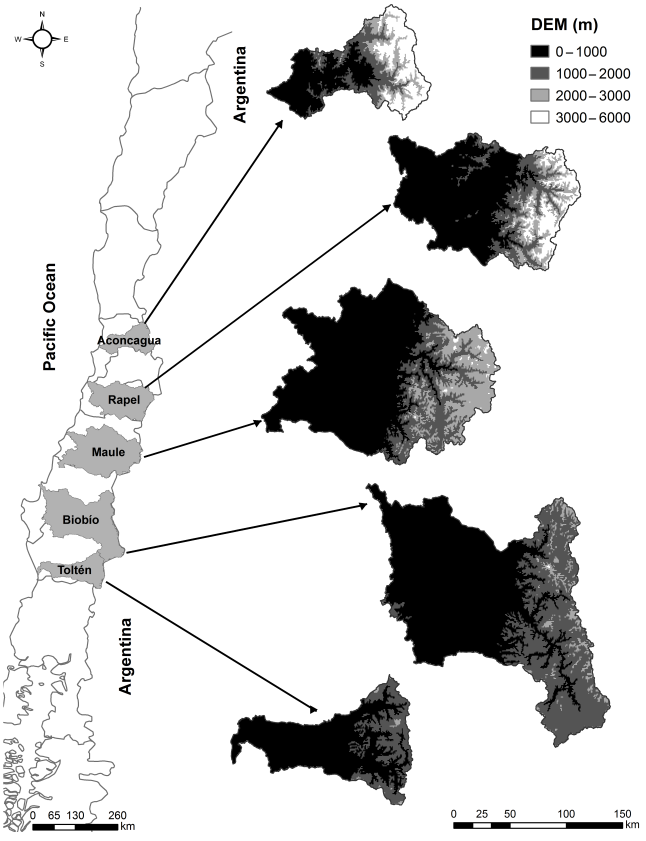

Figure 1. Study sites.

2 Materials and methods

2.1 Study sites

The study site includes five watersheds located in central and southern Chile: Aconcagua, Rapel, Maule, Biobío and Toltén (Fig. 1). The watersheds were chosen considering their population and dependence on water-resourced economic activities.

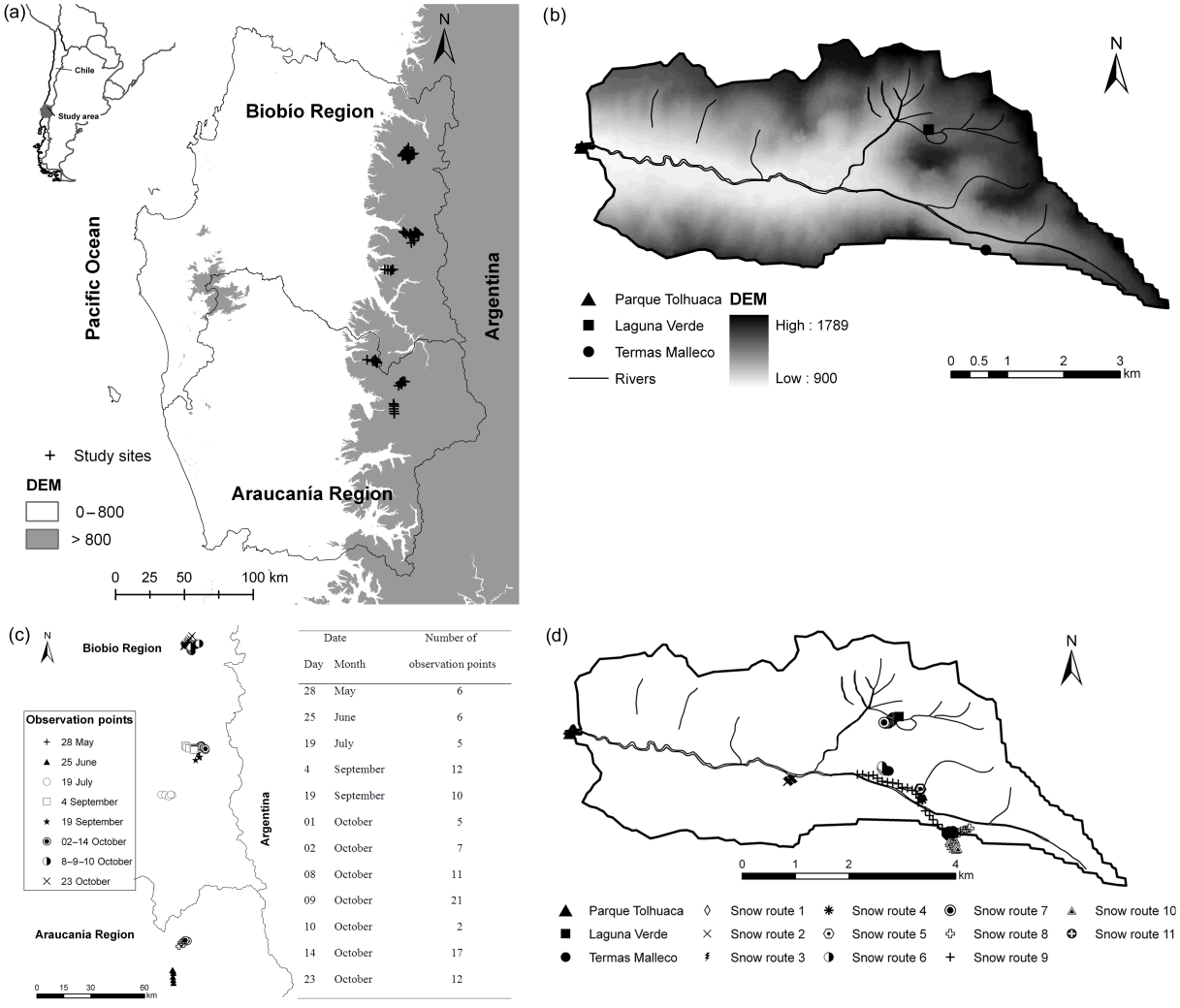

Figure 2. **(a)** Study sites for MOD10A2 validation. **(b)** Location of the meteorological stations for continuous monitoring of snow depth. **(c)** Location and date of 1-day observation points. **(d)** Location of the snow courses.

The Aconcagua watershed is located in the Valparaiso region, between the parallels 32°14′–33°09′ S and 69°59′–71°33′ W, with an area of 7340 km^2 and a maximum elevation of 5843 m a.s.l. Approximately 40 % of the watershed lies above the snowline (average altitude above which snow can be found in winter), which is located at 2100 m (Garreaud, 1992). The climate in the watershed is temperate Mediterranean with a long dry season of 7 to 8 months and a wet season of approximately 4 months (May–August) during which more than 80 % of the precipitation occurs. The average annual precipitation is 529 mm. Principal economic activities at the watershed are agriculture, mining and industries. It has a population of around 600 000 inhabitants (4 % of the Chilean population).

The Rapel watershed is located in the General Libertador Bernardo O'Higgins region between the parallels 33°52′–35°00′ S and 70°00′–71°53′ W, with an area of 13 695 km^2 and a maximum elevation of 5138 m a.m.s.l. Approximately 30 % of the watershed lies above the snowline which is located at 1500 m (Peña and Vidal, 1993). The climate in the watershed is temperate Mediterranean, with a dry season of 4 to 5 months (November–March) and a wet season of approximately 4 months (May–August) during which more than 75 % of the precipitation occurs. The average annual precipitation is 960 mm. The main economic activities at the watershed are agriculture and mining. It has a population of around 570 000 inhabitants (3.8 % of the Chilean population).

The Maule watershed is located in the Maule region, between the parallels 35°05′–36°35′ S and 70°18′–72°42′ W, with an area of 20 295 km^2 and a maximum elevation of 3931 m a.m.s.l. Approximately 32 % of the watershed lies above the snowline, which is located at 1150 m (Peña and Vidal, 1993). The climate in the watershed is temperate Mediterranean, with a 6-month dry season (November–

April) and a wet season of approximately 4 months (May–August) during which more than 75 % of the precipitation occurs. The average annual precipitation is 1471 mm. The main economic activity at the watershed is agriculture. It has a population of around 410 000 inhabitants (2.7 % of the Chilean population).

The Biobío watershed is located in the Biobío region, between the parallels 36°45′–38°49′ S and 71°00′–73°20′ W, with an area of 24 264 km^2 and a maximum elevation of 3487 m a.m.s.l. Approximately 41 % of the watershed lies above the snowline, which is located at 850 m (Peña and Vidal, 1993). The climate in the watershed is Mediterranean, with a 5-month dry season (November–March) and a wet season of approximately 4 months (May–August), during which more than 55 % of the precipitation occurs. The average annual precipitation is 1891 mm. Principal economic activities related to water resources at the watershed are agriculture, forestry and industries. It has a population of around 630 000 inhabitants (4.2 % of the Chilean population).

The Toltén watershed is located in the Araucanía region, between the parallels 38°32′–39°38′ S and 71°21′–73°16′ W, with an area of 8398 km^2 and a maximum elevation of 3710 m a.m.s.l. Approximately 37 % of the watershed lies above the snowline, which is located at 750 m (Peña and Vidal, 1993). The climate in the watershed is temperate rainforest with Mediterranean influence, characterized by precipitation throughout the year but having less rain during the summer months than in the winter ones. The average annual precipitation is 2870 mm. Main economic activities related to water resources at the watershed are tourism, agriculture and forestry. It has a population of around 170 000 inhabitants (1.1 % of the Chilean population).

2.2 Ground observations of SCA

For validation of MOD10A2, ground observations were performed, including continuous monitoring of snow depth with meteorological stations, snow courses, and 1-day observations of snow presence and depth at some mountain trails. Figure 2a shows the locations of measuring sites.

2.2.1 Continuous monitoring of snow depth

In order to perform a continuous measurement of snow depth, three meteorological stations were installed in the upper part of the Biobío watershed. The stations are Parque Tolhuaca, located at 900 m a.s.l., Termas Malleco at 1190 m a.s.l., and Laguna Verde at 1410 m a.s.l. Also, snow depth data from three DGA meteorological stations (Portillo, 3005 m a.s.l., Laguna Negra, 2709 m a.s.l., and Volcan Chillan, 1964 m a.s.l.) were used. Figure 2b shows the location of the meteorological stations.

Snow depth was measured using acoustic snow depth sensors (Campbell Scientific, SR50A) with a frequency of 15 min. Corrections for variation of the speed of sound in air were made considering the air temperature measured at the same time intervals as the snow depth, using the temperature and relative humidity probe (Vaisala, HMP60). The data were collected from April 2010 to December 2011 at the Termas Malleco station, and from July 2011 to December 2011 at the Parque Tolhuaca and Laguna Verde stations. In the case of the DGA station, available data from April 2013 to December 2015 were used. Snow data were grouped considering the average snow depth over 8 days (same 8-day period of MOD10A2) and then reclassified as snow (1) if the average snow depth was >0 cm and as no-snow (0) for snow depth $= 0$ cm.

Table 1. Dates and repetition times for each snow route during winter 2011.

Snow route	Dates	No. of times route was repeated
1	30 Jun	1
2	30 Jun	1
3	30 Jun, 19 Jul, 31 Aug, 14 Sep	4
4	1 Jul, 19 Jul, 31 Aug, 15 Sep	4
5	1 Jul	1
6	1 Jul	1
7	1 Jul	1
8	31 Aug, 15 Sep	2
9	1 Sep, 15 Sep	2
10	31 Aug, 14 Sep	2
11	31 Aug, 14 Sep	2

2.2.2 One-day observation points

To cover a large spatial domain and to achieve a better spatial and temporal representation of SCA, a total of 124 different single measurements of snow depth were conducted during field campaigns at different mountain trails. Field measurements were taken from the end of June until the beginning of October 2011. The location of each observation point was recorded with a GPS and snow depth was measured with a Black Diamond QuickDraw Tour Probe 190. Figure 2c shows the location of the observation points and the date and number of observations for each day.

2.2.3 Snow courses

During 6 days of the 2011 winter season, 11 snow courses were conducted in the upper Malleco watershed. Figure 2d shows the location of snow courses. Each route was recorded with a GPS. Snow depth and density were measured with a Black Diamond QuickDraw Tour Probe 190 and Snow Sampling Tubes (3600 Federal Snow Tubes, Standard-Metric), respectively. Table 1 shows the dates and repetitions for each snow route performed.

2.3 MODIS snow cover products

The Moderate Resolution Imaging Spectroradiometer (MODIS) is on the Earth Observing System, which employs a cross-track scan mirror and a set of individual detector elements to provide imagery of the Earth's surface and clouds in 36 discrete and narrow spectral bands ranging in wavelength from 0.405 to 14.385 µm. It provides medium-to-coarse resolution imagery with a high temporal repeat cycle (1–2 days). The main purpose of the MODIS is to facilitate the study of global vegetation and land cover, vegetation properties, global land surface changes, surface albedo, surface temperature as well as snow and ice cover, on a daily or nearly daily basis. The MODIS snow cover products are one of the many geophysical standard products derived from MODIS data. The MODIS snow cover products are provided on a daily basis (MOD10A1) and as 8-day composites (MOD10A2), both at 500 m resolution over the Earth's land surfaces. MOD10A1 consists of 1200 km by 1200 km tiles of 500 m resolution data gridded in a sinusoidal map projection and MOD10A2 is a composite of MOD10A1 especially produced to show maximum snow extent. For this study, MOD10A2v005 (Hall et al., 2016) was used. Classification of SCA using MODIS collected data was done based on the Normalized Difference Snow Index (NDSI) (Hall et al., 1995; Klein et al., 1998; Riggs et al., 2006). Images were reprojected to WGS84 UTM 19S using the MODIS Reprojection Tool (MRT).

MODIS estimates of SCA were validated for the period between April 2010 and December 2011 by comparing them with ground observations. Eighty snow maps from MOD10A2 were analysed. Only cloud-free observations for each cell of the map grid were used.

2.4 Validation of MOD10A2

To validate the correspondence between the image classification and ground observations, a confusion matrix was used (Congalton and Mead, 1983; Story and Congalton, 1986, 1991; Foody, 2002). The confusion matrix is a simple cross tabulation of classified data versus observed ones, providing a basis for accuracy assessment (Campbell, 1996; Canters, 1997). Figure 3 presents the confusion matrix and how the different indexes were calculated.

2.5 Assessment of SCD

SCA variation in the five selected watersheds was evaluated using MOD10A2 for the period covering the years 2000–2016 using a total of 774 images. All images were processed in ArcGis, reprojecting them to WGS84 19S and cut according to the desired area, in this case for the Aconcagua, Rapel, Maule, Biobío and Toltén watersheds. SCA and clouds were quantified for each available image, and annual and seasonal averages of snow cover were calculated for each watershed.

SCD was analysed through a number of statistical tests to explore observed trends in SCA during the study period. "Non-parametric" statistical tests were chosen because they are more robust than the "parametric" test. A Mann–Kendall test was applied to determine the existence of monotonic trends. Sen's method (Gilbert, 1987) was applied to determine the rate of observed changes.

An analysis of the correlation between SCA and mean annual precipitation for the upper part of the watershed was done. Considering the spatial location of SCA, only precipitation stations located over the 700 m a.s.l. were considered. Availability of daily precipitation was evaluated for each year at each station; only years with more than 80 % of data were used in order to obtain the mean annual precipitation. The precipitation for the watershed was obtained considering the arithmetic mean between available stations. Table 2 shows the stations that were used and the availability of data.

3 Results

The MOD10A2 product was validated for determination of SCA in the watersheds under study and the SCD was analysed.

3.1 Validation of MOD10A2 through ground observations

The composite images MOD10A2 were compared with ground observations. For the study period 23, 75, 26, 119, 123 and 32 images were available for comparison with observations at Parque Tolhuaca, Termas Malleco, Laguna Verde, Portillo, Laguna Negra and Volcan Chillan stations, respectively. Clouds were present in 2 (9 %), 1 (1 %), 1 (4 %), 3 (3 %), 3 (2 %) and 2 (6 %) images for each aforementioned station, respectively. Table 3 presents the confusion matrix and the indexes of agreement. Overall accuracies of 86, 81, 88, 92, 83 and 97 % were observed at Parque Tolhuaca, Termas Malleco, Laguna Verde, Portillo, Laguna Negra and Volcan Chillan stations, respectively, which reached the target of 85 % (Thomlinson et al., 1999).

A total of 117 images corresponding to the study period were available for comparison with 1-day observations, with none of them classified as covered by "clouds". All ground observations were done over areas with snow presence. When comparing it to MOD10A2 images, the agreement was 97 %. MODIS that did not coincide with ground observations occurred during the beginning of the snowfall season or at the end of the melting period. In both cases, snow patches were observed in the field, covering areas at the subpixel scale of the MOD10A2 image.

For comparison with snow courses, a total of 282 images were available during the study period, all of them without clouds. Ground observations were done on areas covered by

k,k	A	B	C	...	q	$\sum$
A	n_{AA}	n_{AB}	n_{AC}	...	n_{Aq}	n_{A+}
B	n_{BA}	n_{BB}	n_{BC}	...	n_{Bq}	n_{B+}
C	n_{CA}	n_{CB}	n_{CC}	...	n_{Cq}	n_{C+}
⋮	⋮	⋮	⋮	...	⋮	⋮
q	n_{qA}	n_{qB}	n_{qC}	...	n_{qq}	n_{q+}
$\sum$	n_{+A}	n_{+B}	n_{+C}	...	n_{+q}	n

$$\text{Percentage correct} = \frac{\sum_{k=1}^{q} n_{kk}}{n} \times 100$$

$$\text{User's accuracy} = \frac{n_{kk}}{n_{k+}} \times 100$$

$$\text{Producer's accuracy} = \frac{n_{kk}}{n_{+k}} \times 100$$

Figure 3. Confusion matrix and percentage correct (overall accuracy), user accuracy and producer accuracy.

Table 2. Precipitation stations and availability of data.

Watershed	Station	Elevation m a.s.l.	Number of years with more than 80 % of data	% of availability
Aconcagua	Resguardo Los Patos	1220	16	98 %
	Rio Putaendo En Resguardo Los Patos	1218	11	81 %
	Jahuel	1020	15	97 %
	Los Andes	820	16	100 %
	Rio Aconcagua En Chacabuquito	950	16	100 %
	Vilcuya	1100	16	100 %
	Riecillos	1290	16	100 %
	Las Chilcas	850	16	98 %
Rapel	Rio Pangal En Pangal	1500	13	86 %
	Rio Cachapoal 5 km. Aguas Abajo Junta Cortaderal	1127	12	88 %
	Central Las Nieves	700	5	35 %
	La Rufina	743	16	99 %
Maule	Fundo El Radal	685	16	99 %
	Vilches Alto	1058	16	100 %
	Hornillo	810	16	99 %
	Rio Melado En El Salto	730	12	78 %
Biobío	Embalse Ralco	742	5	35 %
	Rio Biobío En Llanquen	767	11	74 %
	Laguna Malleco	894	14	96 %
	Liucura	1043	16	98 %
Toltén	Lago Tinquilco	850	16	100 %
	Puesco (Aduana)	620	14	94 %

snow only. The overall accuracy of MOD10A2 for predicting SCA was 98 %.

Results indicate that MOD10A2 has a satisfactory agreement with ground observations, and therefore the 8-day composite images are suitable for analysis of SCD in the Andean watersheds.

3.2 Assessment of SCD

Figure 4 shows the SCD in Aconcagua, Rapel, Maule, Biobío and Toltén watersheds for the period 2000–2016. All watersheds show the same SCD with more SCA in winter than the other seasons. It can be appreciated that in the Maule, Biobío and Toltén watersheds the maximum SCA in 2016 is considerably lower than in the 5 previous years, and is one of the lowest of the whole study period.

Figure 5 shows mean SCA for each season and annual precipitation in the Aconcagua, Rapel, Maule, Biobío and Toltén watersheds for the period 2000–2016. Northern watersheds, i.e. Aconcagua and Rapel, present a higher SCA percentage. It can be appreciated that years with more precipitation do not necessarily have more SCA; instead, years with lower

Table 3. Confusion matrix and indexes of agreement for Parque Tolhuaca, Termas Malleco and Laguna Verde stations.

		Ground observation								
		Parque Tolhuaca Station			Termas Malleco Station			Laguna Verde Station		
		snow	no-snow	User's accuracy	snow	no-snow	User's accuracy	snow	no-snow	User's accuracy
MOD10A2	Snow	6	2	0.75	22	13	0.63	16	1	0.94
	no-snow	1	12	0.92	1	38	0.97	2	6	0.75
Producer's accuracy		0.86	0.86		0.96	0.75		0.89	0.86	
Overall accuracy		0.86			0.81			0.88		
		Ground observation								
		Portillo Station			Laguna Negra Station			Volcan Chillan Station		
		snow	no-snow	User's accuracy	snow	no-snow	User's accuracy	snow	no-snow	User's accuracy
MOD10A2	Snow	43	7	0.86	45	0	1.00	11	1	0.92
	no-snow	2	64	0.97	21	54	0.72	0	18	1.00
Producer's accuracy		0.96	0.90		0.68	1.00		1.00	0.95	
Overall accuracy		0.92			0.93			0.97		

precipitation have a higher SCA. Figure 6 displays the relation between SCA and annual precipitation for the different watersheds; it is clear that only at Aconcagua is there a good adjustment to the regression line ($R^2 = 0.7$) with a positive slope. In Rapel and Maule we can see a positive relation but with R^2 smaller than 0.5, which indicates a deficient adjustment. At Biobío we can graphically see a negative slope, i.e. when there is more precipitation there is less SCA, but statistically we have no adequate adjustment.

Figure 7 shows the variability of spatial distribution of maximum yearly SCA for the five watersheds. Years with maximum and minimum SCA of yearly maximum SCA are not coincident between watersheds. A considerable spatial variability of maximum SCA can be appreciated. There are no trends in the data.

Figure 8 shows annual and seasonal trends of SCA at the Aconcagua, Rapel, Maule, Biobío and Toltén watersheds. Trend analysis of the SCA series was performed with the non-parametric Mann–Kendall test. Decreasing trends in annual mean SCA are observed (p-value < 0.01) for the Aconcagua and Rapel watersheds, with a decreasing slope of $30\,\mathrm{km^2\,yr^{-1}}$ (Fig. 8a, b). No significant annual trend was observed for the other three watersheds. In autumn (Fig. 8a), only the Aconcagua watershed shows a decreasing trend of mean SCA variation at a level of significance $\leqq 0.05$, with a decreasing slope of $54\,\mathrm{km^2\,yr^{-1}}$. There is no significant variation in SCA in the winter (Fig. 8). In spring (Fig. 8b, c) the Rapel and Maule watersheds have a decreasing trend at a level of significance $\leqq 0.05$, with a decreasing slope of 38 and $79\,\mathrm{km^2\,yr^{-1}}$, respectively. In summer (Fig. 8c), the Rapel watershed has a decreasing trend at a level of significance $\leqq 0.05$, with a slope of $24\,\mathrm{km^2\,yr^{-1}}$; the Aconcagua and Maule watersheds show some decreasing trends with level of significance $\leqq 0.1$ and slopes of 10 and $11\,\mathrm{km^2\,yr^{-1}}$ (Fig. 8a, c). It is important to remark that the Rapel watershed has large glacier areas. All the above-mentioned results are coincident with the outcomes given by the Pettitt homogeneity test, which shows that time series are not homogenous between two given times (p-value < 0.01). The change in the average in most of the cases is observed between 2008 and 2011.

Considering snow accumulation and melt seasons, data were grouped in two periods, i.e. autumn–winter (accumulation) and spring–summer (melt). For these two periods, a trend analysis was also done. Results indicated that there is a negative trend in average SCA during both seasons; the Aconcagua watershed has a decreasing slope (p-value < 0.01) of $29\,\mathrm{km^2\,yr^{-1}}$ during the snow accumulation season and the Maule watershed has a decreasing slope (p-value < 0.05) of $26\,\mathrm{km^2\,yr^{-1}}$ during the melt season. In the case of yearly maximum SCA, we found a significant positive trend for the Biobío watershed (p-value < 0.01); the other watersheds show a non-significant linear trend.

4 Discussion

In general terms, we can say that MOD10A2 has good agreement with ground observations, with always over 80 % precision when the sky is clear. Our results are a bit lower than the 90 % obtained in studies of the Northern Hemisphere (Zhou et al., 2005; Liang et al., 2008a; Wang et al., 2008; Huang et al., 2011; Zheng et al., 2017); this difference can be attributed to the complex topography of the Chilean Andes. Greater disagreements between MOD10A2 and ground observations were found at Termas Malleco and Laguna Negra stations. These stations are located close to the snowline where most

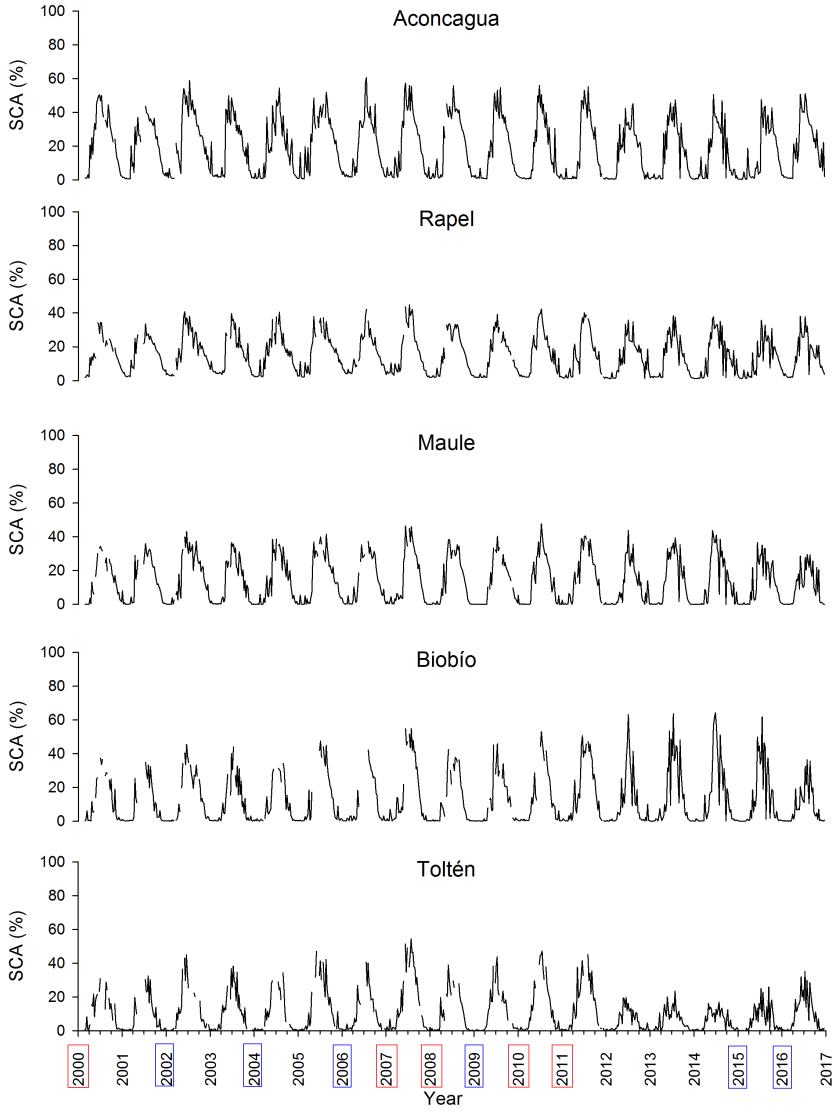

Figure 4. SCD for the 2000–2016 period at Aconcagua, Rapel, Maule, Biobío and Toltén watersheds. Red boxes indicate Niña years, blue ones Niño years.

of the time the soil is not covered by snow or is covered by snow for small periods of time; in this case, the presence of small snow patches is expected to be highly variable in time; it can even change at the subdaily scale and therefore it could reduce the capacity of images to capture snow coverage in the proximity of the snowline. Regarding SCA, we can see in the results presented in Figs. 4 and 5 that SCA has a similar behaviour in the different watersheds during the study period, i.e. all watersheds follow the same snow accumulation and melt dynamics and the maximum and minimum % of SCA are also coincident in time. SCA has a strong inter-annual variability, which is in agreement with the results obtained by other studies (Masiokas et al., 2006; Marchane et al., 2015; Tang et al., 2013; Zhang et al., 2012). Comparing the result with those obtained by Karici et al. (2016) in Slovak watersheds, we can appreciate similar results for the Aconcagua, Rapel and Maule watersheds and opposite ones for Biobío and Toltén, i.e. for the 2001–2006 period a decrease in mean SCA with respect to the mean of the whole period, and more SCA for the period 2007–2012.

Comparing our results of SCA with those of SWE obtained by Cornwell et al. (2016), we can appreciate that they are in agreement only with respect to the years 2002 and 2005 displaying the largest SCA of the entire study period. The other results are in dissension, as we have more years with above mean SCA during the beginning of the study period, and below throughout the end of the period (2012–2016).

In the case of trend analysis only the watersheds located in the northern part of the study area have a significant de-

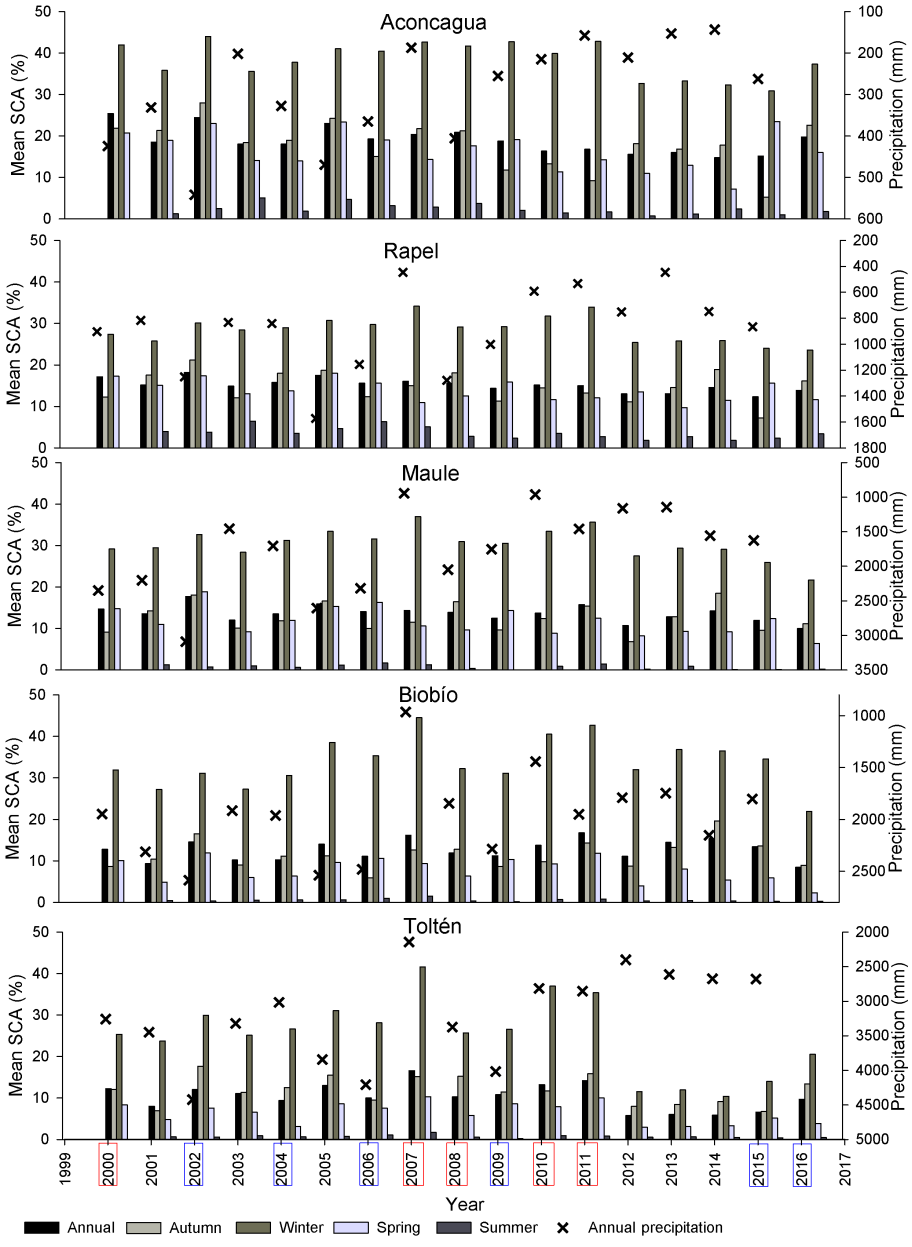

Figure 5. Mean seasonal and annual SCA (%) in Aconcagua, Rapel, Maule, Biobío and Toltén watersheds during 2000–2016. Red boxes indicate Niña years, blue ones Niño years.

creasing trend during accumulation and melt season, which is in agreement with results from different studies in Asia and North America (Tang et al., 2013; Maskey et al., 2011; Gurung et al., 2017; Fassnacht and Hultstrand, 2015; Kunkel et al., 2016). During wintertime we could not see any significant trend, which is consistent with results from Dietz et al. (2012).

The SCA magnitude for each watershed was contrasted with historical data from El Niño/La Niña–Southern Oscillation (ENSO) episodes from 2000 to 2016[1]. Normal or neutral years correspond to historical conditions, as Niño and Niña years correspond to wet and dry years, respectively, in the case of central and southern Chile. During 2000 and 2016, five episodes of El Niño (2002, 2004–2005, 2006–2007, 2009 and 2015–2016) and three episodes of La Niña (1999–2000, 2007–2008 and 2010–2011) occurred. Niño and Niña episodes were defined using the Oceanic Niño Index (ONI).

[1] http://www.cpc.noaa.gov/products/analysis_monitoring/ensostuff/ensoyears.shtml

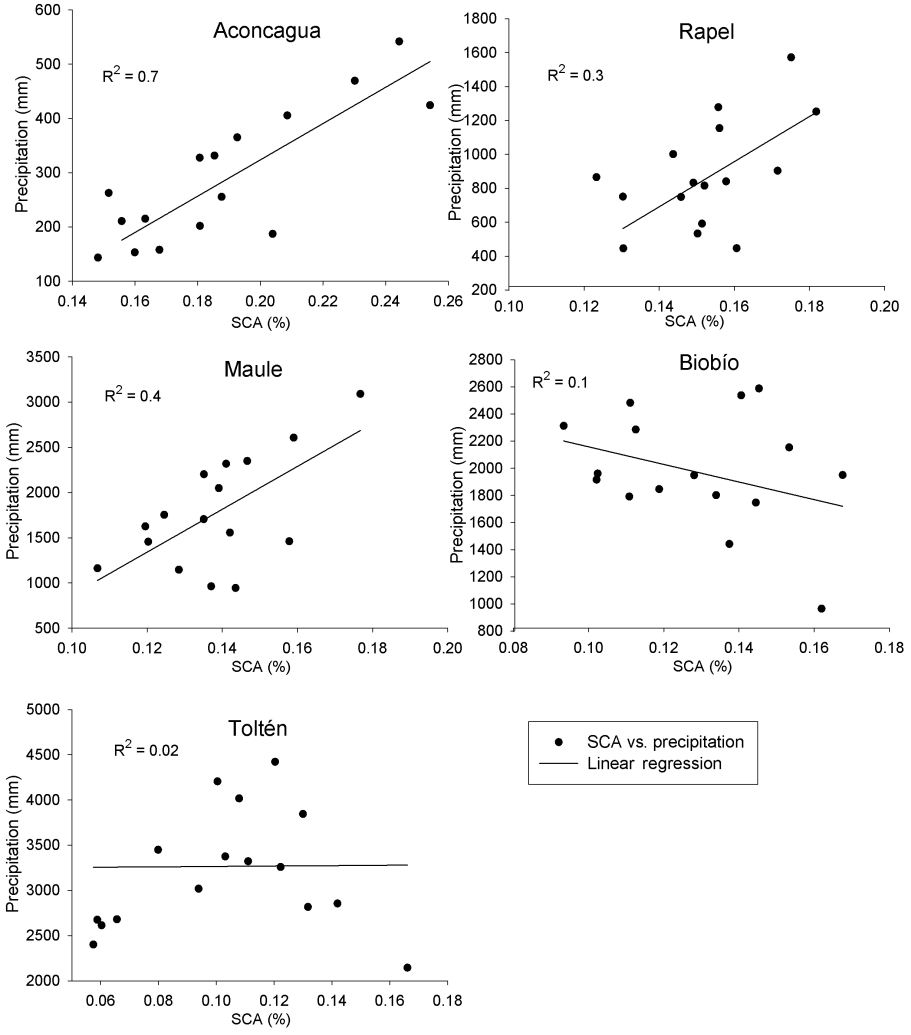

Figure 6. Relation between % of mean annual SCA and annual precipitation at Aconcagua, Rapel, Maule, Biobío and Toltén watersheds.

Niña years are coincident with maximum SCA in wintertime in all watersheds, with similar amounts of SCA between different Niña episodes. The 2007 Niña event is coincident with the highest % of SCA during winter for the study period (2000–2016) in all watersheds. Winter SCAs for Niña and Niño episodes are all above or just at the mean SCA for the 14 years under study. Years under the mean of the SCA area are all not coincident with Niña and Niño episodes, i.e. normal years are all under the mean SCA value. There is also no linear relation between the amount of precipitation and SCA, with the exception of the Aconcagua watershed (Fig. 6). This study only analysed snow coverage and not snow depth, i.e. volume of snow, which implies that a bigger SCA is not necessarily related to more water stored as snow. Considering the existing data availability in time and space of the DGA regarding snow depth, it was not possible to carry out an analysis of changes in snow depth in this study. During the course of the last 5 years, an important decline in SCA was perceived in the entire watershed, with the exception of the Biobío watershed, where no difference can be seen until the last year (2016). This decline is bigger at the Toltén watershed, where the average for the last 5 years is 50 % of the mean for the entire period. In the analysis of the precipitation data we can observe that in all watersheds there was a rainfall deficit during 2012–2016: Aconcagua 26 %, Rapel 29 %, Maule 24 %, Biobío 19 %, and Toltén 27 % (DGA, 2012, 2013, 2014, 2015, 2016; DMC, 2013, 2014).

Masiokas et al. (2006) studied snowpack variation between 1951 and 2005 in Chile between latitude 30 and 37° S. They found that snow accumulation is positively related to El Niño, but they could not find a clear relationship with La Niña. The correlations that they found between snowfall and annual amount of rainfall in central Chile fit well with the known positive correlation of precipitation with El Niño during the Southern Hemisphere winter (June–August) (Waylen and Caviedes, 1990; Montecinos and Aceituno, 2003). It

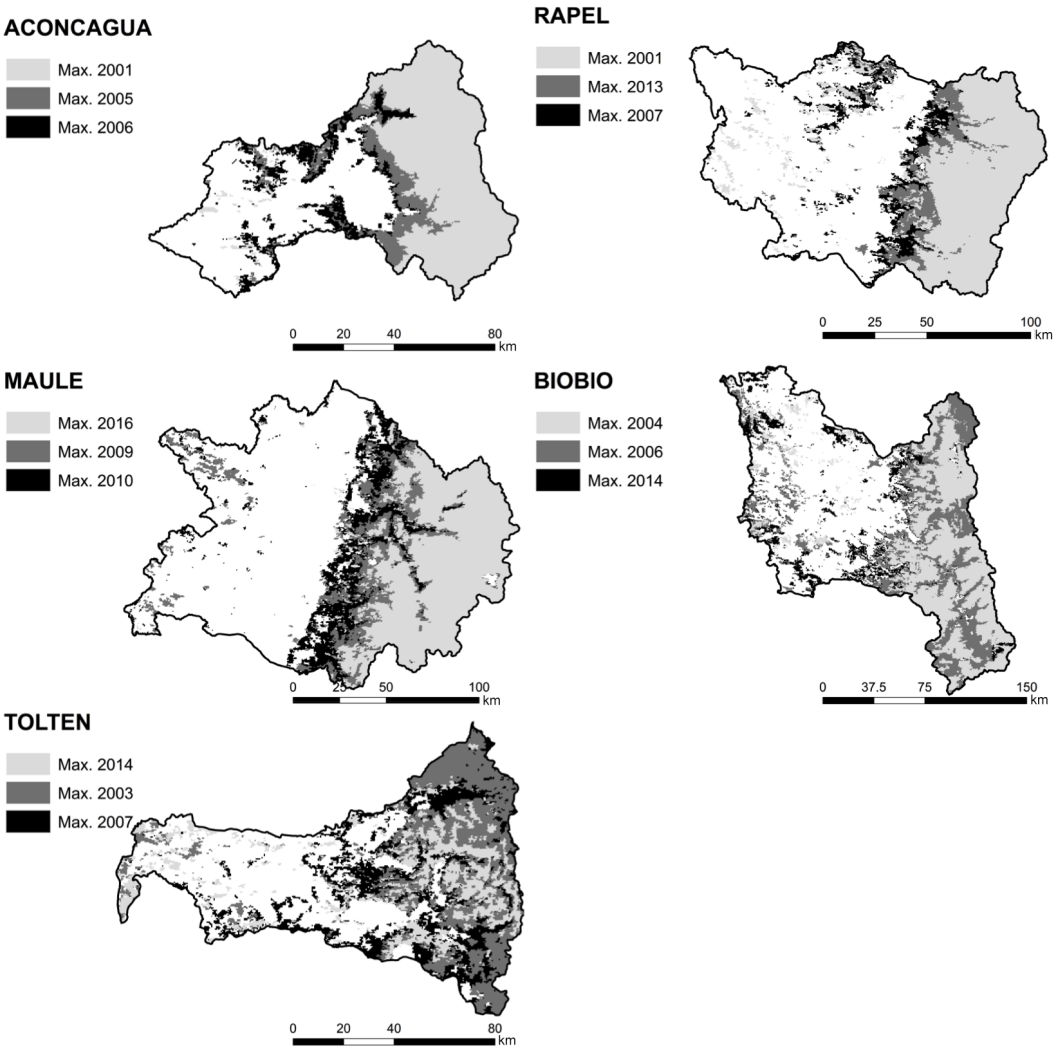

Figure 7. Spatial representation of SCA for the period 2000–2016 in Aconcagua, Rapel, Maule, Biobío and Toltén watersheds. Black indicates the year with maximum SCA, dark grey the year with average SCA and grey the year with minimum SCA.

came to their attention that, in contrast to the decreasing trend in snowpack observed across western North America, in the region they studied the average regional maximum value of snow water equivalent shows a positive to non-significant trend. In our case, we have only analysed SCA, obtaining a decreasing trend in the watersheds located in the northern part (32.0–36° S) and, to the south, a non-significant trend (35–39.5° S). These results are in agreement with the ones obtained by Falvey and Garreaud (2009), who noticed that, in central and northern Chile (17–37° S), in situ temperature observations confirm warming in the central valley and western Andes ($+0.25\,^{\circ}\mathrm{C\,decade^{-1}}$). In southern Chile (38–48° S) temperature trends over land are weak (insignificant at 90 % confidence).

In the watersheds located south of 35° S we observed no relation between SCA and annual precipitation, which is in agreement with the results of Cortés et al. (2011), who found that all watersheds they studied that were located north of 35° S had a high and significant correlation with ONI, and that precipitation during El Niño and La Niña episodes seems to be the most important factor controlling the water year hydrograph centre of timing, but with no influence in the southern ones.

5 Conclusions

The first validation of MODIS snow product MOD10A2 for estimation of snow covered areas (SCAs) via remote sensing in watersheds located in the Southern Hemisphere was presented. Ground observations of SCA were conducted during the years 2010 and 2011 at six study sites including six meteorological stations, 124 1-day single-observation points, and 11 snow courses. The SCA was determined for 636 days from MODIS snow products and compared with the SCA

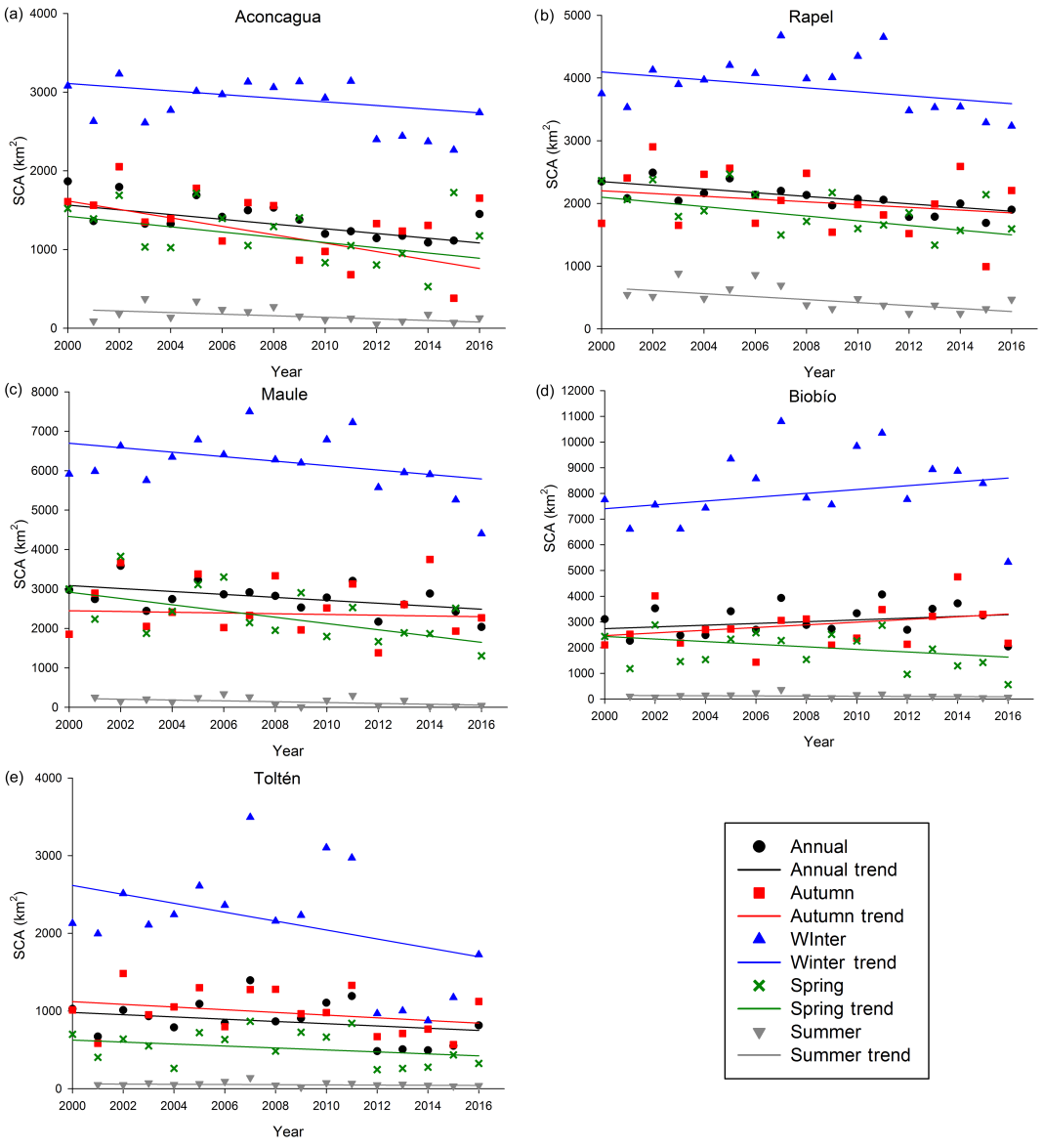

Figure 8. Annual and seasonal trends of SCA at Aconcagua, Rapel, Maule, Biobío and Toltén watersheds.

measured in situ. The SCA estimated from MOD10A2 presented an overall agreement from 81 to 98 % with SCA determined from ground observations, showing that the MODIS snow product can be taken as a feasible remote sensing tool for SCA estimation in southern–central Chile.

On the other side, we have analysed SCA trends for the period 2000–2016 in five of the most important watersheds of southern–central Chile in the context of water use and inhabitants, covering a longitudinal gradient from 32°14′ to 39°38′ S, which implies different climates regarding precipitation, drier in the northern part than in the southern part. Results indicate that all watersheds have the same SCD with more snow during wintertime, which decreases during spring and summer. Furthermore, a significant negative trend in annual mean SCA is observed for the Aconcagua and Rapel watersheds, which can have implications for water availability for summertime. In general, we can see that there is no significant reduction in SCA for 2000–2016, with the exception of the Aconcagua watershed. From the data we can appreciate an important decline in SCA for the period of 2012 to 2016, which is coextensive with the rainfall deficit that occurred during the same years.

Results were compared with the ENSO episode during 2000–2016. From the latter comparison we can conclude that in the previously mentioned period, Niña years are coincident with maximum SCA at wintertime in all watersheds, with similar amounts of SCA between different Niña episodes.

In summary, the results presented in this work are highly relevant and can be used as one feasible approximation to obtain SCA, particularly in the Chilean Andes because of the lack of hydrological data such as discharge data, snow courses, and snow depths. These can become an outstanding tool to improve the analysis of important hydrological processes and the validation of water quantity prediction models.

Data availability. MOD10A2 are available from (https://reverb.echo.nasa.gov/reverb). Meteorological data are available from the DGA website (http://www.dga.cl/servicioshidrometeorologicos/Paginas/default.aspx), and self-generated data are available in the supplement below.

The Supplement related to this article is available online at https://doi.org/10.5194/hess-21-5111-2017-supplement.

Competing interests. The authors declare that they have no conflict of interest.

Acknowledgements. The present research was conducted in the framework of the FONDECYT 11100119 project.

Edited by: Stefan Uhlenbrook
Reviewed by: three anonymous referees

References

Aulta, T. W., Czajkowski, K. P., Benko, T., Coss, J., Struble, J., Spongberg, A., Templin, M., and Gross, C.: Validation of the MODIS snow product and cloud mask using student and NWS cooperative station observations in the Lower Great Lakes Region, Remote Sens. Environ., 105, 341–353, 2006.

Ayala, A., McPhee, J., and Vargas, X.: Altitudinal gradients, midwinter melt, and wind effects on snow accumulation in semiarid midlatitude Andes under La Niña conditions, Water Resour. Res., 50, 3589–3594, 2014.

Azmat, M., Umar Liaqat, U. W., Muhammad Uzair Qamar, M. U., and Awan, U. K.: Impacts of changing climate and snow cover on the flow regime of Jhelum River, Western Himalayas, Reg. Environ. Change, 17, 813–825, 2017.

Barnett, T. P., Adam, J. C., and Lettenmaier, D. P.: Potential impacts of a warming climate on water availability in snow-dominated regions, Nature, 438, 303–309, 2005.

Boegh, E., Thorsen, M., Butts, M. B., Hansen, S., Christiansen, J. S., Abrahamsen, P., Hasager, C. B., Jensen, N. O., van der Keur, P., Refsgaard, J. C., Schelde, K., Soegaard, H., and Thomsen, A.: Incorporating remote sensing data in physically based distributed agro-hydrological modeling, J. Hydrol., 287, 279–299, 2004.

Campbell, J. B.: Introduction to remote sensing, 2nd Edn., London, Taylor and Francis, 1996.

Canters, F.: Evaluating the uncertainty of area estimates derived from fuzzy land-cover classification, Photogramm. Eng. Rem. S., 63, 403–414, 1997.

Congalton, R.: A review of assessing the accuracy of classifications of remotely sensed data, Remote Sens. Environ., 37, 35–46, 1991.

Congalton, R. and Mead, R.: A quantitative method to test for consistency and correctness in photointerpretation, Photogramm. Eng. Rem. S., 49, 69–74, 1983.

Cornwell, E., Molotch, N. P., and McPhee, J.: Spatio-temporal variability of snow water equivalent in the extra-tropical Andes Cordillera from distributed energy balance modeling and remotely sensed snow cover, Hydrol. Earth Syst. Sci., 20, 411–430, 2016.

Cortés, G., Vargas, X., and McPhee, J.: Climatic sensitivity of streamflow timing in the extratropical western Andes Cordillera, J. Hydro, 405, 93–109, 2011.

Demaria, E. M. C., Maurer, E. P., Thrasher, B., Vicuña, S., and Meza, F. J.: Climate change impacts on an alpine watershed in Chile: Do new model projections change the story?, J. Hydrol., 502, 128–138, 2013.

DGA: Manual de Cálculo de Crecidas y Caudales Mínimos en Cuencas Sin Información Fluviométrica, 1995.

DGA: Información pluviométrica, fluviométrica, estado de embalses y aguas subterráneas, ssd no. 6423872, Boletín no. 416 diciembre, 2012.

DGA: Información pluviométrica, fluviométrica, estado de embalses y aguas subterráneas, ssd no. 7429039, Boletín no. 428 diciembre, 2013.

DGA: Información pluviométrica, fluviométrica, estado de embalses y aguas subterráneas, ssd no. 8441530, Boletín no. 440 diciembre, 2014.

DGA: Información pluviométrica, fluviométrica, estado de embalses y aguas subterráneas, ssd no. 9490165, Boletín no. 452 diciembre, 2015.

DGA: Información pluviométrica, fluviométrica, estado de embalses y aguas subterráneas, ssd no. 10557841, Boletín no. 464 diciembre, 2016.

Dietz, A., Wohner, C., and Kuenzer, C.: European Snow Cover Characteristics between 2000 and 2011 Derived from Improved MODIS Daily Snow Cover Products, Remote Sens., 4, 2432–2454, https://doi.org/10.3390/rs4082432, 2012.

DMC: Dirección General de Aeronáutica Civil Dirección Meteorológica e Chile. Subdepartamento Climatología y Met. Aplicada, Anuario Climatológico 2012 Santiago–Chile 2013, 2013.

DMC: Dirección General de Aeronáutica Civil Dirección Meteorológica e Chile. Subdepartamento Climatología y Met. Aplicada, Anuario Climatológico 2013 Santiago–Chile 2014, 2014.

Er-Raki, S., Chehboun, A., and Duchemin, B.: Combining Satellite Remote Sensing Data with the FAO-56 Dual Approach for Water Use Mapping In Irrigated Wheat Fields of a Semi-Arid Region, Remote Sens., 2, 375–387, 2010.

Escobar, F. and Aceituno, P.: Influencia del fenómeno ENSO sobre la precipitación nival en el sector andino de Chile central durante el invierno, Bull. Inst. Fr. Etudes Andines, 27, 753–759, http://documentos.dga.cl/MET1074.pdf, 1998.

Falvey, M. and Garreaud, R.: Regional cooling in a warming world: Recent temperature trends in the southeast Pacific and along the west coast of subtropical South

America (1979–2006), J. Geophys. Res., 114, D04102, https://doi.org/10.1029/2008JD010519, 2009.

Fassnacht, S. R. and Hultstrand, M.: Snowpack variability and trends at long-term stations in northern Colorado, USA, Proceedings of the International Association of Hydrological Sciences, 371, 131–136, 2015.

Foody, G. M.: Status of Land Cover Classification Accuracy Assessment, Remote Sens. Environ., 80, 185–201, https://doi.org/10.1016/S0034-4257(01)00295-4, 2002.

Garreaud, R.: Estimación de la línea de nieve en cuencas de Chile Central, Rev. Soc. Chilena Ing. Hidráulica, Revista de la Sociedad Chilena de Ingeniería Hidráulica, 7, 21–32, 1992.

Garreaud, R.: Warm winter storms in Central Chile, J. Hydrometeorol., 14, 1515–1534, 2013.

Gilbert, R. O.: Statistical methods for environmental pollution monitoring, Van Nostrand Reinhold, New York, 1987.

Gurung, D. R., Maharjan, S. B., Shrestha, A. B., Shrestha, M. S., Bajracharya, S. R., and Murthy, M. S. R.: Climate and topographic controls on snow cover dynamics in the Hindu Kush Himalaya, Int. J. Climatol., 37, 3873–3992, https://doi.org/10.1002/joc.4961, 2017.

Hall, D. K. and Riggs, G. A.: Accuracy assessment of the MODIS snowcover products, Hydrol. Process., 21, 1534–1547, 2007.

Hall, D. K., Riggs. G. A., and Salomonson, V. V.: Development of methods for mapping global snow cover using bloderate Resolution Imaging Spectroradiometer (MODIS) data, Remote Sew. Environ., 54, 127–140, 1995.

Hall, D. K., Riggs, G. A, Salomonson, V. V., Di Girolamo, N. E., and Bayr, K. J.: MODIS snow-cover products, Remote Sens. Environ., 83, 181–194, 2002.

Hall, D. K., Riggs, G. A., and Salomonson, V.: Updated weekly.MODIS/Terra Snow Cover 8-day L3 Global 500 m Grid 15 V005, 24 February 2000–31 December 2016, Boulder, Colorado USA, National Snow and Ice Data Center, Digital media, 2016.

Harpold, A. A., Brooks, P. D., Rajogopal, S., Heidebuchel, I., Jardine, A., and Stielstra, C.: Changes in snowpack accumulation and ablation in the intermountain west, Water Resour. Res., 48, W11501, https://doi.org/10.1029/2012WR011949, 2012.

Huang, X. D., Liang, T. G., Zhang, X. T., and Guo, Z. G.: Validation of MODIS snow cover products using Landsat and ground measurements during the 2001–2005 snow seasons over northern Xinjiang, China, Int. J. Remote Sens., 32, 133–155, 2011.

Klein, A. G. and Barnett, A. C.: Validation of daily MODIS snow cover maps of the Upper Rio Grande River Basin for the 2000–2001 snow year, Remote Sens. Environ., 86, 162–176, 2003.

Kuchment, L. S., Romanov, P., Gelfan, A. N., and Demidov, V. N.: Use of satellite-derived data for characterization of snow cover and simulation of snowmelt runoff through a distributed physically based model of runoff generation, Hydrol. Earth Syst. Sci., 14, 339–350, https://doi.org/10.5194/hess-14-339-2010, 2010.

Kunkel, K., Robinson, D. A., Champion, S., Yin, X., Estilow, T., and Frankson, R.: Trends and Extremes in Northern Hemisphere Snow Characteristics, Curr. Clim. Change Rep., 2, 65–73, https://doi.org/10.1007/s40641-016-0036-8, 2016.

Krajcí, P., Holko, L., and Parajka, J.: Variability of snow line elevation, snow cover area and depletion in the main Slovak basins in winters 2001–2014, J. Hydrol. Hydromech., 64, 12–22, 2016.

Lee, S., Klein, A. G., and Over, T. M.: A Comparison of MODIS and NOHRSC Snow-Cover Products for Simulating Streamflow using the Snowmelt Runoff Model, Hydrol. Process., 19, 2951–2972, 2006.

Li, H.-Y. and Wang, J.: Simulation of snow distribution and melt under cloudy conditions in an Alpine watershed, Hydrol. Earth Syst. Sci., 15, 2195–2203, https://doi.org/10.5194/hess-15-2195-2011, 2011.

Liang, T., Huang, X., Wu, C., Liu, X., Li, W., Guo, Z., and Ren, J.: Application of MODIS data on snow cover monitoring in pastoral area: a case study in the Northern Xinjiang, China, Remote Sens. Environ., 112, 1514–1526, 2008a.

Marchane, A., Jarlan, L., Hanich, L., Boudhar, A., Gascoinb, S., Tavernier, A., Filali, N., Le Page, M., Hagolle, O., and Berjamy, B.: Assessment of daily MODIS snow cover products to monitor snow cover dynamics over the Moroccan Atlas mountain range, Remote Sens. Environ., 160, 72–86, 2015.

Masiokas, M., Villalba, R., Luckman, B., Le Quesne, C., and Aravena, J. C.: Snowpack Variations in the Central Andes of Argentina and Chile, 1951–2005: Large-Scale Atmospheric Influences and Implications for Water Resources in the Region, J. Clim., 19, 6334–6352, 2006.

Maskey, S., Uhlenbrook, S., and Ojha, S.: An analysis of snow cover changes in the Himalayan region using MODIS snow products and in-situ temperature data, Climatic Change, 108, 391–40, 2011.

Melesse, A. M., Weng, Q. H., Thenkabail, P. S., and Senay, G. B.: Remote sensing sensors and applications in environmental resources mapping and modeling, Sensors, 7, 3209–3241, 2007.

Meza, F. J., Wilks, D. S., Gurovich, L., and Bambach, N.: Impacts of climate change on irrigated agriculture in the Maipo Basin, Chile: reliability of water rights and changes in the demand for irrigation, J. Water Res. Pl.-ASCE, 138, 421–430, 2012.

Milzowa, C., Kgotlhan, L., Kinzelbach, W., Meier, P., and Bauer-Gottwein, P.: The role of remote sensing in hydrological modelling of the Okavango Delta, Botswana, J. Environ. Manage., 90, 2252–2260, 2009.

Montecinos, A. and Aceituno, P.: Seasonality of the ENSO-related rainfall variability in central Chile and associated circulation anomalies, J. Clim., 16, 281–296, 2003.

Montzka, C., Canty, M., Kunkel, R., Menz, G., Vereecken, H., and Wendland, F.: Modelling the water balance of a mesoscale catchment basin using remotely sensed land cover data, J. Hydrol., 353, 322–334, 2008.

Pederson, G. T., Betancourt, J. L., and McCabe, G. J.: Regional patterns and proximal causes of the recent snowpack decline in the Rocky Mountains, US, Geophys. Res. Lett., 40, 1811–1816, 2013.

Peña, H. and Vidal, F.: Estimación Estadística de la Línea de Nieves durante los Eventos de Precipitación entre las latitudes 28 y 38 grados Sur, XI Congreso Chileno de Ingeniería Hidráulica, Concepción, Chile, 1993.

Ragettli, S., Cortés, G., McPhee, J., and Pellicciotti, F.: An evaluation of approaches for modelling hydrological processes in high-elevation, glacierized Andean watersheds, Hydrol. Process., 28, 5674–5695, 2013.

Riaño, D., Chuvieco, E., Salas, J., and Aguado, I.: Assessment of Different Topographic Corrections in Landsat-TM Data for Map-

ping Vegetation Types, IEEE T. Geosci. Remote, 41, 1056–1061, 2003.

Riggs, G. A., Hall, D. K., and Salomonson, V. V.: MODIS Snow Products User Guide to Collection 5, Online article, retrieved on 2 January 2007 at: http://modis-snow-ice.gsfc.nasa.gov/userguides.html, 2006.

Simic, A., Fernandes, R., Brown, R., Romanov, P., and Park, W.: Validation of Vegetation, MODIS, and GOES Plus SSM/I Snow-Cover Products Over Canada Based on Surface Snow Depth Observations, Hydrol. Process., 18, 1089–1104, 2004.

Snehmani, J. K. D., Kochhar, I., Hari Ram, R. P., and Ganju, A.: Analysis of snow cover and climatic variability in Bhaga basin located in western Himalaya, Geocarto Inter., 31, 1094–1107, 2016.

Stehr, A., Debels, P., Arumi, J. L., Romero, F., and Alcayaga, H.: Combining the Soil and Water Assessment Tool (SWAT) and MODIS imagery to estimate monthly flows in a data-scarce Chilean Andean basin, Hydrolog. Sci. J., 54, 1053–1067, 2009.

Stehr, A., Aguayo, M., Link, O., Parra, O., Romero, F., and Alcayaga, H.: Modelling the hydrologic response of a mesoscale Andean watershed to changes in land use patterns for environmental planning, Hydrol. Earth Syst. Sci., 14, 1963–1977, https://doi.org/10.5194/hess-14-1963-2010, 2010.

Story, M. and Congalton, R. G.: Accuracy assessment: a user's perspective, Photogramm. Eng. Rem. S., 52, 397–399, 1986.

Tang, Z., Wang, J., Li, H., and Yan, L.: Spatiotemporal changes of snow cover over the Tibetan plateau based on cloud-removed moderate resolution imaging spectroradiometer fractional snow cover product from 2001 to 2011, J. App. Remote Sens., 7, 1–14, 2013.

Tekeli, A. E., Akyürek, Z., Sorman, A. A., Sensoy, A., and Sorman, A. Ü.: Using MODIS snow cover maps in modeling snowmelt runoff process in the eastern part of Turkey, Remote Sens. Environ., 97, 216–230, 2005.

Thomlinson, J. R., Bolstad, P. V., and Cohen, W. B.: Coordinating methodologies for scaling landcover classification from site-specific to global: steps toward validating global maps products, Remote Sens. Environ., 70, 16–28, 1999.

Valdés-Pineda, R., Pizarro, R., García-Chevesich, P., Valdés, J. B., Olivares, C., Vera, M., and Abarza, A.: Water governance in Chile: Availability, management and climate change, J. Hydrol., 519, 2538–2567, 2014.

Verbunt, M., Gurtz, J., Jasper, K., Lang, H., Warmerdam, P., and Zappa, M.: The hydrological role of snow and glaciers in alpine river basins and their distributed modeling, J. Hydrol., 282, 36–55, 2003.

Vicuña, S., Garreaud, R., and McPhee, J.: Climate change impacts on the hydrology of a snowmelt driven basin in semiarid Chile, Climatic Change, 105, 469–488, 2011.

Vicuña, S., McPhee, J., and Garreaud, R.: Agriculture Vulnerability to Climate Change in a Snowmelt Driven Basin in Semiarid Chile, J. Water Res. Pl.-ASCE, 138, 431–441, 2012.

Vicuña, S., Gironás, J., Meza, F. J., Cruzat, M. L., Jelinek, M., Bustos, E., Poblete, D., and Bambach, N.: Exploring possible connections between hydrological extreme events and climate change in central south Chile, Hydrolog. Sci. J., 58, 1598–1619, 2013.

Wang, W., Huang, X., Deng, J., Xie, H., and Liang, T.: Spatio-Temporal Change of Snow Cover and Its Response to Climate over the Tibetan Plateau Based on an Improved Daily Cloud-Free Snow Cover Product, Remote Sens., 7, 169–194, 2015.

Wang, X., Xie, H., and Liang, T.: Evaluation of MODIS Snow Cover and Cloud Mask and its Application in Northern Xinjiang, China, Remote Sens. Environ., 112, 1497–1513, 2008.

Waylen, P. R. and Caviedes, C. N.: Annual and seasonal fluctuations of precipitation and streamflow in the Aconcagua River basin, J. Hydrol., 120, 79–102, 1990.

Zeinivand, H. and De Smedt, F.: Simulation of snow covers area by a physical based model, World Academy of Science, Engineering and Technology, 55, 469–474, 2009.

Zhang, G., Xie, H., Yao, T., Liang, T., and Kang S.: Snow cover dynamics of four lake basins over Tibetan Plateau using time series MODIS data (2001–2010), Water Resour. Res., 48, W10529, https://doi.org/10.1029/2012WR011971, 2012.

Zheng, W., Du, J., Zhou, X., Song, M., Bian, G., Xie, S., and Feng, X.: Vertical distribution of snow cover and its relation to temperature over the Manasi River Basin of Tianshan Mountains, Northwest China, J. Geogr. Sci., 27, 403–419, https://doi.org/10.1007/s11442-017-1384-6, 2017.

Zhou, X., Xie, H., and Hendrickx, M. H. J.: Statistical evaluation of remotely sensed snow-cover products with constraints from streamflow and SNOTEL measurements, Remote Sens. Environ., 94, 214–231, 2005.